Development 137, 3215-3220 (2010) doi:10.1242/dev.052225

Hand2 ensures an appropriate environment for cardiac fusion by limiting Fibronectin function

Zayra V. Garavito-Aguilar[1,2], Heather E. Riley[2] and Deborah Yelon[1,2,*]

SUMMARY

Heart formation requires the fusion of bilateral cardiomyocyte populations as they move towards the embryonic midline. The bHLH transcription factor Hand2 is essential for cardiac fusion; however, the effector genes that execute this function of Hand2 are unknown. Here, we provide in zebrafish the first evidence for a downstream component of the Hand2 pathway that mediates cardiac morphogenesis. Although *hand2* is expressed in cardiomyocytes, mosaic analysis demonstrates that it plays a non-autonomous role in regulating cardiomyocyte movement. Gene expression profiles reveal heightened expression of *fibronectin 1* (*fn1*) in *hand2* mutant embryos. Reciprocally, overexpression of *hand2* leads to decreased Fibronectin levels. Furthermore, reduction of *fn1* function enables rescue of cardiac fusion in *hand2* mutants: bilateral cardiomyocyte populations merge and exhibit improved tissue architecture, albeit without major changes in apicobasal polarity. Together, our data provide a novel example of a tissue creating a favorable environment for its morphogenesis: the Hand2 pathway establishes an appropriate environment for cardiac fusion through negative modulation of Fn1 levels.

KEY WORDS: Zebrafish, Heart morphogenesis, Lateral plate mesoderm, Hand2, Fibronectin

INTRODUCTION

To create the embryonic heart tube, bilateral groups of cardiomyocytes move towards the midline, merge through a process called cardiac fusion, and organize into a cylinder (Bakkers et al., 2009; Schoenebeck and Yelon, 2007). The regulation of these cell behaviors requires a combination of the qualities of the extracellular environment that facilitate cell behavior and the inherent traits of the cardiomyocytes that control their motility. However, the mechanisms that coordinate extrinsic and intrinsic influences on morphogenesis remain poorly understood.

Mutations that disrupt cardiomyocyte movement have revealed several extracellular requirements for cardiac fusion. For example, cardiac fusion depends upon cues from the endoderm: in zebrafish and mouse, mutations that disrupt anterior endoderm specification inhibit fusion, causing two separate hearts to form in lateral positions, a condition known as cardia bifida (e.g. Kuo et al., 1997; Molkentin et al., 1997; Reiter et al., 1999). Additionally, cardia bifida is caused by mutations that disrupt sphingosine-1-phosphate signaling, which is essential for the integrity of the anterior endoderm (Kupperman et al., 2000; Osborne et al., 2008). Furthermore, the presence of the extracellular matrix (ECM) has a potent influence on cardiomyocyte movement. Inhibition of Fibronectin (Fn) function in zebrafish, mouse or chick causes cardia bifida (George et al., 1997; Linask and Lash, 1988; Trinh and Stainier, 2004), as does the impairment of ECM assembly due to loss of function of the proteoglycan Syndecan 2 (Arrington and Yost, 2009).

Cell-intrinsic factors also contribute to the regulation of cardiomyocyte movement. For example, the myocardial transcription factor Hand2 plays a key role during cardiac fusion: in zebrafish *hand2* mutants, small clusters of cardiomyocytes appear trapped bilaterally (Yelon et al., 2000). This cardia bifida phenotype does not result from endodermal defects, as the anterior endoderm appears normal in *hand2* mutants (Wendl et al., 2007). However, the *hand2* mutant myocardium exhibits abnormal epithelial polarity and disorganized Fn deposition (Trinh et al., 2005). These defects appear unrelated to the reduced number of cardiomyocytes in *hand2* mutants because embryos lacking *gata5* have a similarly small number of cardiomyocytes and do not exhibit problems with polarity or Fn deposition (Trinh et al., 2005). It is not yet clear whether regulation of cardiomyocyte movement by Hand2 is a consequence of its role in myocardial polarization or its role in ECM deposition. Moreover, it is not known which effector genes downstream of Hand2 execute its morphogenetic functions. Although a few myocardial differentiation genes are known to be regulated by Hand2 [e.g. α-*MHC*, *Irx4*, *Nppa* (Bruneau et al., 2000; Dai et al., 2002; Thattaliyath et al., 2002)], none of these appears to be relevant to its role in cardiac fusion.

Here, we provide the first genetic link between Hand2 and a downstream effector by which it mediates morphogenesis. Mosaic analysis demonstrates that the influence of *hand2* on cardiomyocyte movement is not cell autonomous. Furthermore, we find an inverse relationship between *hand2* and *fibronectin 1* (*fn1*) function: *hand2* mutants exhibit heightened *fn1* expression, and overexpression of *hand2* reduces levels of Fn. Increased Fn1 function appears responsible for inhibition of cardiomyocyte movement in *hand2* mutants: reduction of *fn1* levels can rescue cardiac fusion in the absence of *hand2*. Together, our data provide a novel example of a tissue creating an appropriate environment for its own morphogenesis: the Hand2 pathway establishes a favorable milieu for cardiac fusion through negative regulation of Fn1 function.

[1]Division of Biological Sciences, University of California, San Diego, La Jolla, CA 92093, USA. [2]Developmental Genetics Program and Department of Cell Biology, Kimmel Center for Biology and Medicine, Skirball Institute of Biomolecular Medicine, New York University School of Medicine, New York, NY 10016, USA.

*Author for correspondence (dyelon@ucsd.edu)

Accepted 16 July 2010

MATERIALS AND METHODS

Zebrafish

The following zebrafish strains were used: *han*^{s6} (Yelon et al., 2000), *nat*^{tl43c} (Trinh and Stainier, 2004), *Tg(myl7:egfp)*^{twu277} (Huang et al., 2003) and *Tg(myl7:dsredt4)*^{sk74}, a stable line carrying a previously described transgene (Auman et al., 2007).

Transplantation

Blastomere transplantation was performed as described previously (Thomas et al., 2008). Donor and host embryos carried either *Tg(myl7:egfp)* or *Tg(myl7:dsredt4)*, facilitating distinction of cardiomyocyte origins. Intercrosses of *han* heterozygotes were used to generate donor or host embryos as appropriate. When necessary, donors were retained for genotyping. Confocal images of mosaic embryos were obtained using a Zeiss LSM510 microscope and analyzed with Volocity software (Improvision).

Microarrays and qRT-PCR

Gene expression profiles from wild-type and *han* mutant embryos at 19 hours post-fertilization (hpf) were compared using Affymetrix zebrafish GeneChips. Examination of *Tg(myl7:egfp)* expression allowed sorting of *han* mutant embryos from their wild-type siblings. For each microarray, we extracted 3-9 μg of RNA from 10-25 embryos using the RNeasy Kit (Qiagen). Triplicate samples were processed by the Genomics Core Laboratory at the Memorial Sloan-Kettering Cancer Center, and clustering analysis was performed using ArrayAssist software (Stratagene). For validation of results, we extracted RNA using the RNAqueous-4PCR Kit (Ambion), synthesized cDNA using the iScript Kit (Bio-Rad), performed quantitative (q) RT-PCR using SYBR Green with the iCycler system (Bio-Rad), and analyzed the data using the comparative C_T method (Schmittgen and Livak, 2008). Microarray data have been deposited at the GEO repository with accession number GSE23381.

Injection

Embryos were injected at the one-cell stage with 200 pg *hand2* mRNA (Yelon et al., 2000) or 2.5 ng of anti-*apkci* morpholino (Rohr et al., 2006).

Immunofluorescence

Embryos were fixed in 4% paraformaldehyde for 1 hour at room temperature. Following cryosectioning (10 μm), antibody staining was performed as described previously (Trinh and Stainier, 2004) using the following antibodies: rabbit anti-Fn (Sigma F3648), 1:100; rabbit anti-aPKC (Santa Cruz Biotechnology SC-216), 1:1000; mouse anti-β-catenin (Sigma C7207), 1:500; and mouse anti-ZO-1 (Zymed 33-9100), 1:200. Secondary antibodies were goat anti-mouse Alexa Fluor 594 and 647 and goat anti-rabbit Alexa Fluor 594 and 647 (Molecular Probes). Confocal images were obtained using Zeiss LSM510 and Leica SP5 microscopes and analyzed with Imaris 6.2 software (Bitplane).

In situ hybridization

In situ hybridization was performed as described previously (Thomas et al., 2008). Images were captured with a Zeiss M2Bio microscope and a Zeiss AxioCam and were processed with Zeiss AxioVision and Adobe Photoshop software.

Genotyping

PCR genotyping for the deletion allele *han*^{s6} was performed as described previously (Yelon et al., 2000). *han*$^{+/+}$ and *han*$^{+/-}$ embryos are indistinguishable by PCR and are therefore labeled as *han*$^{+/?}$. PCR genotyping of *nat*^{tl43c} was performed using primers 5′-TTATCTGGGCAGCACGCTTC-3′ and 5′-CATCCACCACAAT-GTCTCAAAGAG-3′ to generate a 119 bp fragment. Digestion of the mutant allele with *Mse*I creates 55 and 64 bp fragments.

RESULTS AND DISCUSSION

The role of *hand2* during cardiac fusion is not cell autonomous

In zebrafish, *hand2* is expressed throughout the embryonic heart field, and its expression persists in cardiomyocytes as they undergo morphogenesis (Schoenebeck et al., 2007; Yelon et al., 2000). To test whether *hand2* is required in a cell-autonomous fashion for cardiomyocyte movement, we conducted reciprocal transplantation experiments, exchanging blastomeres between wild-type and *hand2* (*han*^{s6}) mutant embryos and assessing the myocardial contributions of donor-derived cells. Strikingly, *han* mutant cells behaved indistinguishably from wild-type cells when transplanted into a wild-type host (Fig. 1A,B). All *han* donor-derived cardiomyocytes moved towards the midline and integrated normally into the heart (Fig. 1A,B,E), suggesting a non-autonomous role for *hand2* during cardiac fusion. The reciprocal experiment yielded compatible results. Wild-type cells behaved like *han* mutant cells when transplanted into a *han* mutant host: wild-type donor-derived cardiomyocytes always clustered laterally with *han* mutant cardiomyocytes and never moved independently towards the midline (Fig. 1C-E). Therefore, the movement of an individual cardiomyocyte depends on *hand2* function in its environment, rather than on the cell-intrinsic expression of *hand2*.

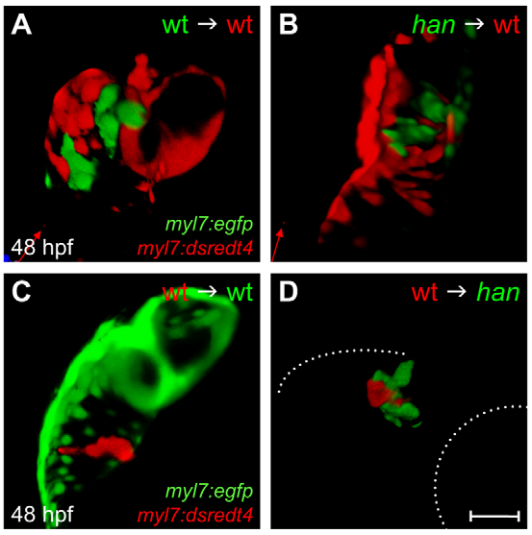

E

Transplant	Transplants with myocardial contribution	Integration into midline heart	Integration into lateral clusters
wt → wt	53/307 (17%)	53	0
han → wt	4/57 (7%)	4	0
wt → wt	33/279 (12%)	33	0
wt → *han*	9/100 (9%)	0	9

Fig. 1. The role of *hand2* in promoting cardiac fusion is not cell autonomous. (**A-D**) Confocal projections of mosaic hearts in live zebrafish embryos. (A-C) Lateral views, dorsal up. (D) Lateral view, dorsal down. (A,B) Wild-type host hearts expressing *Tg(myl7:dsredt4)* with integrated donor-derived cells expressing *Tg(myl7:egfp)* from wild-type (A) or *han* mutant (B) donors. Cells from wild-type or *han* mutant donors integrate indistinguishably into wild-type host hearts. (C,D) Wild-type (C) or *han* mutant (D) hosts expressing *Tg(myl7:egfp)* with integrated wild-type donor-derived cells expressing *Tg(myl7:dsredt4)*. (D) In *han* mutant hosts, wild-type cells behave abnormally, remaining associated with lateral clusters of *han* mutant cardiomyocytes. Only the right-hand cluster is visible in this lateral view. Dotted lines indicate the embryo/yolk border (upper) and eye border (lower). Comparable clusters were observed in all nine chimeras examined, and no donor-derived cardiomyocytes were found outside of the clusters or at the midline. Scale bar: 100 μm. (**E**) Summary of results, indicating the ratio of hosts with donor-derived cardiomyocytes to all host embryos screened and the integration of donor-derived cardiomyocytes into the midline heart or lateral clusters.

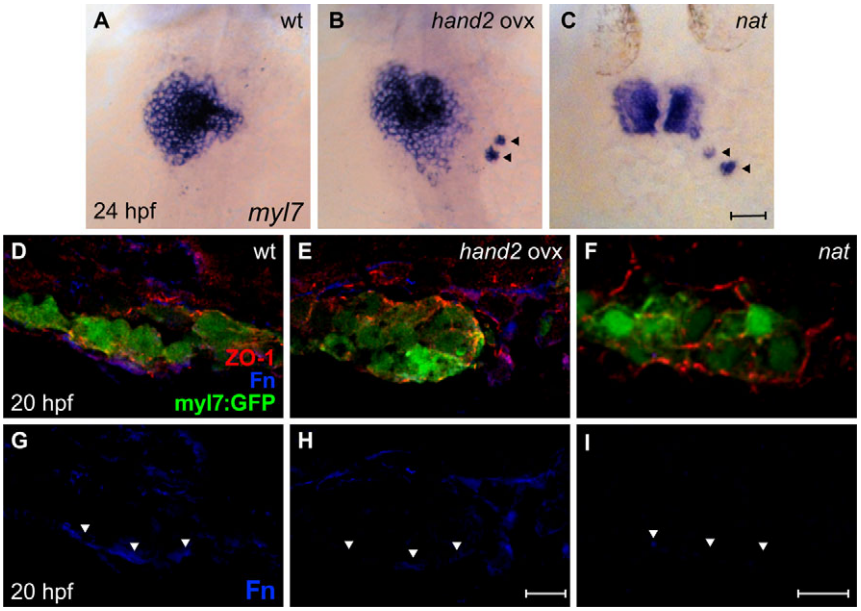

Fig. 2. *hand2* overexpression reduces Fn deposition. (**A-C**) In situ hybridization for *myl7*. Dorsal views, anterior up. Zebrafish embryos overexpressing *hand2* (B) and *nat* mutant embryos (C) exhibit scattered cardiomyocytes (arrowheads), as well as delayed cardiac fusion. (**D-I**) Transverse confocal sections of the left lateral mesoderm in embryos expressing *Tg(myl7:egfp)* (green). Dorsal is up. Immunofluorescence detects ZO-1 (red) and Fn (blue). In contrast to the wild-type monolayer (D), cardiomyocytes are disorganized and multilayered in *hand2*-overexpressing embryos (E) and *nat* mutants (F). Furthermore, the deposition of Fn basal to the myocardium (G, arrowheads) is significantly reduced in *hand2*-overexpressing embryos (H; also see Fig. S2 in the supplementary material) and absent in *nat* mutants (I). Scale bars: 50 μm in A-C; 10 μm in D-I.

It is interesting to note that *han* donor-derived cells became cardiomyocytes less often than wild-type donor-derived cells when transplanted into wild-type hosts (P=0.056, normal approximation of the χ^2 test). The observed ~40% reduction in the frequency of *han* donor-derived myocardial contribution mirrors the ~40% reduction in the production of cardiomyocytes by the *han* mutant heart field (Schoenebeck et al., 2007). By contrast, wild-type donor-derived cells became cardiomyocytes with similar frequencies in wild-type or *han* mutant hosts (P=0.44), suggesting a cell-autonomous function for *hand2* during cardiomyocyte production. Thus, our transplantation data point to the surprising conclusion that the myocardial transcription factor gene *hand2* plays a non-autonomous role in promoting cardiac fusion, seemingly independent of its cell-autonomous role in promoting myocardial differentiation.

The Hand2 pathway limits Fibronectin levels

To identify downstream components of the Hand2 pathway that influence the extracellular environment during cardiac fusion, we used microarrays to compare the gene expression profiles of *han* mutant embryos and their wild-type siblings (see Fig. S1 in the supplementary material). We identified 35 transcripts with a greater than 1.5-fold change in expression level in *han* mutants (see Table S1 in the supplementary material). Nine of these transcripts were downregulated, including *hand2*, *myl7* and *vmhc*, as expected for *han* mutants (Yelon et al., 2000). Among the 26 upregulated transcripts, our attention was drawn to *fn1* (see Fig. S1C in the supplementary material) because of its potential impact on the extracellular environment. Heightened *fn1* expression may contribute to the disorganized Fn deposition in *han* mutants (Trinh et al., 2005), which had not previously been suggested to have a transcriptional basis.

To examine further the relationship between *hand2* function and *fn1* expression, we investigated the effects of *hand2* overexpression. Strikingly, embryos injected with *hand2* mRNA exhibited significant reductions in Fn deposition adjacent to the myocardium and in *fn1* gene expression (Fig. 2D-I and see Fig. S2 in the supplementary material). Fittingly, embryos overexpressing *hand2* also shared several phenotypes with *fn1* mutants [nat^{tl43c} (Trinh and Stainier, 2004)], including delayed cardiac fusion (Fig. 2A-C), occasional scattered cardiomyocytes (Fig. 2B,C), and disorganization of the myocardial monolayer (Fig. 2D-F). Together, the phenotypes of *han* mutants and *hand2*-overexpressing embryos indicate that the Hand2 pathway negatively impacts *fn1* expression levels.

Reduction of *fn1* function rescues cardiac fusion in *hand2* mutants

Our data suggested that *hand2* loss of function could have a non-autonomous effect on cardiac fusion by elevating the levels of Fn in the extracellular environment, thereby inhibiting cardiomyocyte movement. To test this hypothesis, we employed the nat^{tl43c} mutation to reduce *fn1* gene dosage in *han* mutants. Remarkably, heterozygosity for *nat* rescued cardiac fusion in *han* mutants (Fig. 3A,B,E-G,J). In $han^{-/-};nat^{+/-}$ embryos, bilateral populations of cardiomyocytes fused together at the midline (Fig. 3E,J), which never occurred in $han^{-/-}$ mutants (Fig. 3B,G). Although fusion advanced slowly in $han^{-/-};nat^{+/-}$ embryos (Fig. 3A,E,F,J), heart tube assembly did proceed beyond fusion and typically ceased during heart tube extension (Fig. 3O). By contrast, $han^{-/-};nat^{-/-}$ embryos (Fig. 3D,I) exhibited cardia bifida, as in both $han^{-/-}$ and $nat^{-/-}$ embryos (Fig. 3B,C,G,H). Therefore, precise modulation of Fn1 levels is essential to facilitate cardiac fusion. Whereas previous studies have shown that loss of *fn1* hinders cardiomyocyte motility (Trinh and Stainier, 2004), our data show that an excess of *fn1* is similarly deleterious to cardiac fusion. Moreover, the activity of the Hand2 pathway plays a crucial role in preventing excessive Fn1 levels.

We observed a similar trend in the effects of *fn1* gene dosage on a previously unappreciated endocardial defect in $han^{-/-}$ mutants. While myocardial fusion is underway in wild-type embryos, bilateral populations of endocardial cells move towards the midline, where they create an endocardial sheet that gradually shifts leftward as the heart tube extends (Fig. 3P) (Bussmann et al., 2007). In $han^{-/-}$ mutants (Fig. 3Q), the endocardial sheet did not exhibit the same degree of anterior-posterior spreading as in wild-type embryos. Endocardial spreading was also defective in $nat^{-/-}$ and $han^{-/-};nat^{-/-}$ embryos (Fig. 3R,S). However, in $han^{-/-};nat^{+/-}$

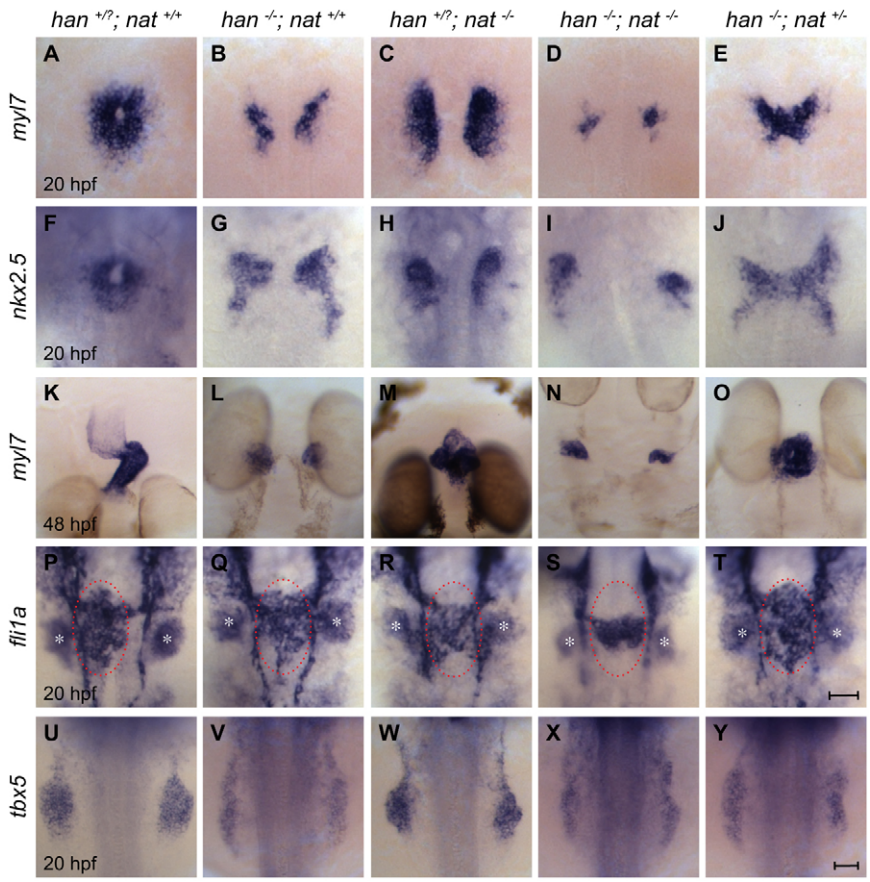

Fig. 3. Reduction of *fn1* function rescues cardiac fusion in *hand2* mutants. In situ hybridizations for the indicated genes. Dorsal views, anterior up. Zebrafish embryos were genotyped by PCR following imaging, and all phenotypes were found to be consistent; for example, the rescue observed in E was seen in a total of 18 embryos from three independent clutches. (**A-J**) Cardiac fusion progresses in wild-type and *han*$^{-/-}$;*nat*$^{+/-}$ embryos, whereas cardia bifida is present in *han*, *nat* and *han*$^{-/-}$;*nat*$^{-/-}$ embryos. (**K-O**) In contrast to the wild-type midline heart, a cardiac cone forms in *han*$^{-/-}$;*nat*$^{+/-}$ embryos, a bifurcated heart forms in *nat* mutants, and cardia bifida is seen in *han* and *han*$^{-/-}$;*nat*$^{-/-}$ embryos. The *nat* cardiac phenotype varies, ranging from a midline heart to cardia bifida (Trinh and Stainier, 2004). (**P-T**) Endocardial sheet formation in wild-type and *han*$^{-/-}$;*nat*$^{+/-}$ embryos contrasts with the dysmorphic endocardium in *han*, *nat* and *han*$^{-/-}$;*nat*$^{-/-}$ embryos. Red ovals mark the extent of anterior-posterior spreading of the endocardial sheet in wild-type and *han*$^{-/-}$;*nat*$^{+/-}$ embryos; this spreading appears inadequate in *han*, *nat* and *han*$^{-/-}$;*nat*$^{-/-}$ embryos, either due to morphogenesis or cell number defects. In addition to its endothelial expression, *fli1a* is expressed in branchial arch mesenchyme (asterisks). (**U-Y**) The failure of pectoral fin mesenchyme development in *han* embryos is not modified by altering *nat* function, in contrast to the normal fin mesenchyme observed in wild-type or *nat* embryos. Scale bars: 50 μm.

embryos, anterior-posterior endocardial spreading appeared to be rescued (Fig. 3T). Thus, the impact of Hand2 function on the levels of Fn in the extracellular environment might explain its effect on the morphogenesis of the endocardium, which lacks *hand2* expression (Schoenebeck et al., 2007).

Despite the amelioration of myocardial and endocardial morphogenesis, not all aspects of the *han* mutant phenotype were rescued in *han*$^{-/-}$;*nat*$^{+/-}$ embryos. For example, *han*$^{-/-}$;*nat*$^{+/-}$ embryos exhibited only a minor improvement in cardiomyocyte production compared with *han*$^{-/-}$ mutants (see Fig. S3 in the supplementary material), consistent with a cell-autonomous role of *hand2* during myocardial differentiation (Fig. 1). Additionally, the forelimb field in *han*$^{-/-}$;*nat*$^{+/-}$ embryos failed to condense into a bud of pectoral fin mesenchyme, just as in *han*$^{-/-}$ mutants (Fig. 3U,V,Y).

Improvement of myocardial fusion and tissue architecture without rescue of epithelial polarity

The arrested heart tube extension in *han*$^{-/-}$;*nat*$^{+/-}$ embryos (Fig. 3O) resembles the cardiac phenotype in zebrafish *apkci* (*heart and soul*; *has*; *prkci* – Zebrafish Information Network) mutants, in which myocardial apicobasal polarity is aberrant (Horne-Badovinac et al., 2001; Peterson et al., 2001). We therefore examined whether the rescue of fusion in *han*$^{-/-}$;*nat*$^{+/-}$ embryos occurs without rescue of the *han*$^{-/-}$ polarity defects. Whereas wild-type cardiomyocytes form an epithelium with basolateral localization of β-catenin, apical distribution of aPKC, lateral localization of ZO-1 (Tjp1 – Zebrafish Information Network) and basal distribution of Fn (Trinh and Stainier, 2004), *han* mutant cardiomyocytes lacked all of these polarized features (Fig. 4D,E,G,H,J,K and see Fig. S4D,E,G,H,J,K in the supplementary material) (Trinh et al., 2005). Furthermore, tissue organization was aberrant in *han* mutants, with dispersed clusters of cardiomyocytes rather than a cohesive monolayer (Fig. 4A,B and see Fig. S4A,B in the supplementary material). In *han*$^{-/-}$;*nat*$^{+/-}$ embryos, myocardial tissue architecture was improved, with cardiomyocytes tending to create a laterally aligned monolayer (Fig. 4C and see Fig. S4C in the supplementary material). Additionally, *han*$^{-/-}$;*nat*$^{+/-}$ cardiomyocytes exhibited improved basal Fn deposition (Fig. 4I,L). However, no other polarized features were rescued in *han*$^{-/-}$;*nat*$^{+/-}$ cardiomyocytes: localization of ZO-1, aPKC and β-catenin was inconsistent and diffuse (Fig. 4F,L and see Fig. S4F,I,L in the supplementary material). Thus, the *han*$^{-/-}$;*nat*$^{+/-}$ phenotype is reminiscent of the effects of *apkci* loss of function, which disrupts multiple indicators of myocardial apicobasal polarity but does not hinder basal Fn deposition (see Fig. S5 in the supplementary material).

It is interesting to note that *apkci* loss of function results in heightened *fn1* expression (see Fig. S5K in the supplementary material), suggesting that the increased *fn1* expression in *han* mutants could be an indirect consequence of myocardial polarity defects. However, the decreased *fn1* expression in embryos overexpressing *hand2* (see Fig. S2D in the supplementary material) indicates that, although polarity defects may contribute to the enhanced *fn1* expression in *han* mutants, it is likely that there is additional complexity to the regulatory relationship between *hand2* and *fn1*. We therefore propose that the Hand2 pathway regulates cardiac morphogenesis through two distinct mechanisms: by limiting Fn levels it controls myocardial cohesion and movement towards the midline; and through independent effectors it establishes the apicobasal polarity that is essential for heart tube extension.

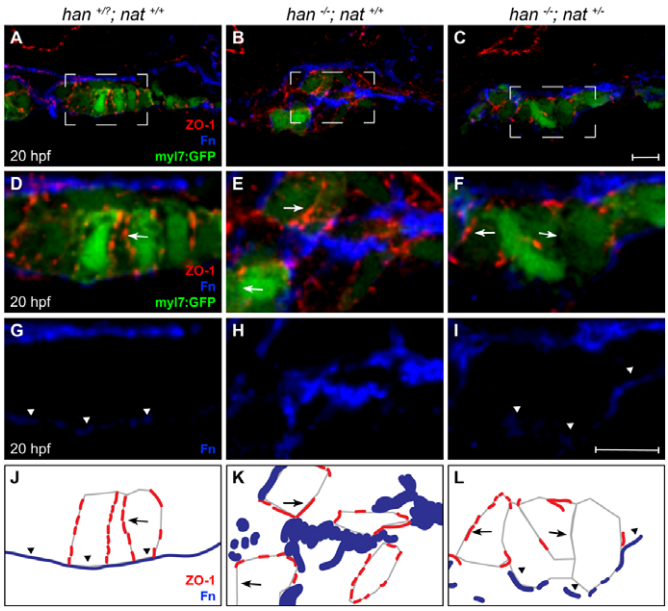

Fig. 4. Tissue architecture and Fn localization improve without rescue of polarity. (**A-I**) Transverse confocal sections of the right lateral mesoderm in zebrafish embryos expressing *Tg(myl7:egfp)* (green). Dorsal is up. ZO-1 (red) and Fn (blue) are detected by immunofluorescence. The boxed regions in A-C are shown at higher magnification in D-I. Scale bars: 10 μm. (**J-L**) Schematics of the cardiomyocyte-associated localization of ZO-1 (red) and Fn (blue) as shown in D-I. Wild-type cardiomyocytes are organized in a cohesive layer (A) and exhibit lateral localization of ZO-1 (D,J, arrows) and basal deposition of Fn (D,G,J, arrowheads). In *han* embryos, tissue architecture is aberrant (B) and myocardial apicobasal polarity is not evident (E,H,K). ZO-1 is diffuse or absent (E,K, arrows) and Fn deposition is disorganized (E,H,K). In $han^{-/-};nat^{+/-}$ embryos, myocardial cohesion (C) and basal Fn localization (F,I,L, arrowheads) are improved, but polarity is not consistently rescued: localization of ZO-1 is either lateral or absent (F,L, arrows).

The Hand2 pathway regulates cardiac morphogenesis by modulating the extracellular environment

Altogether, our data suggest an intriguing model in which cardiomyocytes create an appropriate environment for their own morphogenesis through negative modulation of ECM deposition. Thus, we provide the first evidence that overabundant ECM deposition can be just as detrimental as inefficient ECM deposition to the progress of cardiomyocyte movement. Furthermore, the genetic relationship between *hand2* and *fn1* provides the first demonstration of a downstream component of the Hand2 pathway with a role in determining its cardiac morphogenetic outcomes.

It is interesting to consider the possible mechanisms by which overabundant Fn inhibits cardiac fusion. Excess Fn could create a particularly sticky environment that restricts cell movement. Additionally, high levels of Fn could trigger inappropriate levels of integrin signaling within cardiomyocytes, possibly hindering cell motility. Alternatively, excess Fn might limit the distribution of a diffusible factor that is necessary to stimulate cardiomyocyte movement; a number of factors, such as FGFs (Harada et al., 2009), are dependent upon the ECM for their diffusion, but it is not yet known whether any of these drive cardiac fusion. All of these scenarios would necessitate negative regulation of Fn function in order to advance morphogenesis. In an interesting parallel, a recent study has indicated that gut looping requires Hand2-dependent matrix metalloproteinase activity, suggesting that Hand2 acts to modulate the ECM during multiple aspects of morphogenesis, potentially through different downstream genes (Yin et al., 2010).

In future studies, it will be interesting to address the conservation of the relationship between *hand2* and *fn1*. The role of *Hand2* during cardiac fusion has not been studied in mouse and might be obscured by co-expression of *Hand1* (McFadden et al., 2005). Nevertheless, it is possible that excess Fn could be responsible for the abnormal cardiomyocyte morphology and excessive cardiac jelly that result from conditional deletion of *Hand1* in *Hand2* knockout mice (McFadden et al., 2005). Furthermore, it will be important to determine the molecular nature of the relationship between *hand2* and *fn1*: Hand2 might directly engage *fn1* regulatory regions, which are as yet uncharacterized, or it might influence *fn1* transcription indirectly through additional downstream intermediates. Overall, however direct or indirect, the regulation of Fn levels by the Hand2 pathway provides an appealing paradigm for the means by which a tissue can create the extracellular conditions that pave the way for its morphogenesis.

Acknowledgements

We thank K. Birnbaum, N. Holtzman, H. Knaut, J. Nance, J. Treisman and members of the D.Y. laboratory for critical input; and L. Pandolfo, K. McCrone, E. Reynolds and C. McDaniel for excellent animal care. Work in the D.Y. laboratory is supported by grants from the National Institutes of Health, American Heart Association and March of Dimes. Z.V.G. received support from an American Heart Association Predoctoral Fellowship. Deposited in PMC for release after 12 months.

Competing interests statement

The authors declare no competing financial interests.

Supplementary material

Supplementary material for this article is available at
http://dev.biologists.org/lookup/suppl/doi:10.1242/dev.052225/-/DC1

References

Arrington, C. B. and Yost, H. J. (2009). Extra-embryonic syndecan 2 regulates organ primordia migration and fibrillogenesis throughout the zebrafish embryo. *Development* **136**, 3143-3152.

Auman, H. J., Coleman, H., Riley, H. E., Olale, F., Tsai, H. J. and Yelon, D. (2007). Functional modulation of cardiac form through regionally confined cell shape changes. *PLoS Biol.* **5**, e53.

Bakkers, J., Verhoeven, M. C. and Abdelilah-Seyfried, S. (2009). Shaping the zebrafish heart: from left-right axis specification to epithelial tissue morphogenesis. *Dev. Biol.* **330**, 213-220.

Bruneau, B. G., Bao, Z.-Z., Tanaka, M., Schott, J.-J., Izumo, S., Cepko, C. L., Seidman, J. G. and Seidman, C. E. (2000). Cardiac expression of the ventricle-specific homeobox gene *Irx4* is modulated by Nkx2-5 and dHand. *Dev. Biol.* **217**, 266-277.

Bussmann, J., Bakkers, J. and Schulte-Merker, S. (2007). Early endocardial morphogenesis requires Scl/Tal1. *PLoS Genet.* **3**, e140.

Dai, Y. S., Cserjesi, P., Markham, B. E. and Molkentin, J. D. (2002). The transcription factors GATA4 and dHAND physically interact to synergistically activate cardiac gene expression through a p300-dependent mechanism. *J. Biol. Chem.* **277**, 24390-24398.

George, E. L., Baldwin, H. S. and Hynes, R. O. (1997). Fibronectins are essential for heart and blood vessel morphogenesis but are dispensable for initial specification of precursor cells. *Blood* **90**, 3073-3081.

Harada, M., Murakami, H., Okawa, A., Okimoto, N., Hiraoka, S., Nakahara, T., Akasaka, R., Shiraishi, Y., Futatsugi, N., Mizutani-Koseki, Y. et al. (2009). FGF9 monomer-dimer equilibrium regulates extracellular matrix affinity and tissue diffusion. *Nat. Genet.* **41**, 289-298.

Horne-Badovinac, S., Lin, D., Waldron, S., Schwarz, M., Mbamalu, G., Pawson, T., Jan, Y., Stainier, D. Y. and Abdelilah-Seyfried, S. (2001). Positional cloning of heart and soul reveals multiple roles for PKC lambda in zebrafish organogenesis. *Curr. Biol.* **11**, 1492-1502.

Huang, C. J., Tu, C. T., Hsiao, C. D., Hsieh, F. J. and Tsai, H. J. (2003). Germ-line transmission of a myocardium-specific GFP transgene reveals critical regulatory elements in the cardiac myosin light chain 2 promoter of zebrafish. *Dev. Dyn.* **228**, 30-40.

Kuo, C. T., Morrisey, E. E., Anandappa, R., Sigrist, K., Lu, M. M., Parmacek, M. S., Soudais, C. and Leiden, J. M. (1997). GATA4 transcription factor is required for ventral morphogenesis and heart tube formation. *Genes Dev.* **11**, 1048-1060.

Kupperman, E., An, S., Osborne, N., Waldron, S. and Stainier, D. Y. (2000). A sphingosine-1-phosphate receptor regulates cell migration during vertebrate heart development. *Nature* **406**, 192-195.

Linask, K. K. and Lash, J. W. (1988). A role for fibronectin in the migration of avian precardiac cells. I. Dose-dependent effects of fibronectin antibody. *Dev. Biol.* **129**, 315-323.

McFadden, D. G., Barbosa, A. C., Richardson, J. A., Schneider, M. D., Srivastava, D. and Olson, E. N. (2005). The Hand1 and Hand2 transcription factors regulate expansion of the embryonic cardiac ventricles in a gene dosage-dependent manner. *Development* **132**, 189-201.

Molkentin, J. D., Lin, Q., Duncan, S. A. and Olson, E. N. (1997). Requirement of the transcription factor GATA4 for heart tube formation and ventral morphogenesis. *Genes Dev.* **11**, 1061-1072.

Osborne, N., Brand-Arzamendi, K., Ober, E. A., Jin, S. W., Verkade, H., Holtzman, N. G., Yelon, D. and Stainier, D. Y. R. (2008). The Spinster homologue, Two of Hearts, is required for sphingosine-1-phosphate signaling in zebrafish. *Curr. Biol.* **18**, 1882-1888.

Peterson, R. T., Mably, J. D., Chen, J. N. and Fishman, M. C. (2001). Convergence of distinct pathways to heart patterning revealed by the small molecule concentramide and the mutation heart-and-soul. *Curr. Biol.* **11**, 1481-1491.

Reiter, J. F., Alexander, J., Rodaway, A., Yelon, D., Patient, R., Holder, N. and Stainier, D. Y. (1999). Gata5 is required for the development of the heart and endoderm in zebrafish. *Genes Dev.* **13**, 2983-2995.

Rohr, S., Bit-Avragim, N. and Abdelilah-Seyfried, S. (2006). Heart and soul/PRKCi and nagie oko/Mpp5 regulate myocardial coherence and remodeling during cardiac morphogenesis. *Development* **133**, 107-115.

Schmittgen, T. D. and Livak, K. J. (2008). Analyzing real-time PCR data by the comparative C_T method. *Nat. Protoc.* **3**, 1101-1108.

Schoenebeck, J. J. and Yelon, D. (2007). Illuminating cardiac development: advances in imaging add new dimensions to the utility of zebrafish genetics. *Semin. Cell Dev. Biol.* **18**, 27-35.

Schoenebeck, J. J., Keegan, B. R. and Yelon, D. (2007). Vessel and blood specification override cardiac potential in anterior mesoderm. *Dev. Cell* **13**, 254-267.

Thattaliyath, B. D., Firulli, B. A. and Firulli, A. B. (2002). The basic-helix-loop-helix transcription factor HAND2 directly regulates transcription of the atrial naturetic peptide gene. *J. Mol. Cell. Cardiol.* **34**, 1335-1344.

Thomas, N. A., Koudijs, M., van Eeden, F. J., Joyner, A. L. and Yelon, D. (2008). Hedgehog signaling plays a cell-autonomous role in maximizing cardiac developmental potential. *Development* **135**, 3789-3799.

Trinh, L. A. and Stainier, D. Y. (2004). Fibronectin regulates epithelial organization during myocardial migration in zebrafish. *Dev. Cell* **6**, 371-382.

Trinh, L. A., Yelon, D. and Stainier, D. Y. (2005). Hand2 regulates epithelial formation during myocardial differentiation. *Curr. Biol.* **15**, 441-446.

Wendl, T., Adzic, D., Schoenebeck, J. J., Scholpp, S., Brand, M., Yelon, D. and Rohr, K. B. (2007). Early developmental specification of the thyroid gland depends on han-expressing surrounding tissue and on FGF signals. *Development* **134**, 2871-2879.

Yelon, D., Ticho, B., Halpern, M. E., Ruvinsky, I., Ho, R. K., Silver, L. M. and Stainier, D. Y. (2000). The bHLH transcription factor Hand2 plays parallel roles in zebrafish heart and pectoral fin development. *Development* **127**, 2573-2582.

Yin, C., Kikuchi, K., Hochgreb, T., Poss, K. D. and Stainier, D. Y. R. (2010). Hand2 regulates extracellular matrix remodeling essential for gut-looping morphogenesis in zebrafish. *Dev. Cell* **18**, 973-984.